

# **Photoresponse properties of BaSi<sub>2</sub> epitaxial films grown on the tunnel junction for high-efficiency thin-film solar cells**

Takashi Suemasu, Takanobu Saito, Katsuaki Toh, Atsushi Okada, and Muhammad Ajmal Khan  
Institute of Applied Physics, University of Tsukuba, 1-1-1 Tennohdai, Tsukuba, Ibaraki 305-8573,  
Japan

We have successfully grown 360-nm-thick undoped n-BaSi<sub>2</sub> epitaxial layers on the n<sup>+</sup>-BaSi<sub>2</sub>/p<sup>+</sup>-Si(111) tunnel junction, by molecular beam epitaxy. The external quantum efficiency reached approximately 17.8% at 500 nm under a reverse bias voltage of 4 V at room temperature, the highest value ever reported for semiconducting silicides. The quantum efficiency was compared to 240-nm-thick undoped n-BaSi<sub>2</sub> epitaxial layers on a p-Si(111) substrate.

## 1. Introduction

It is important for solar cell materials to have a large absorption coefficient and a suitable band gap to give a high conversion efficiency. Now, over 90% of solar cells in production are silicon-based. However, the band gap of crystalline Si is as small as 1.1 eV. This value is approximately 0.3 eV smaller than the band gap considered suitable for solar cells. In addition, the optical absorption coefficient  $\alpha$  of crystalline Si is much smaller than that of chalcopyrite semiconductors such as CuGaS<sub>2</sub> and CuInSe<sub>2</sub>. Thus, optical absorption layers of crystalline Si solar cells tend to be much thicker than those of chalcopyrite solar cells. Therefore, novel Si-based materials for high efficiency thin-film solar cells have received great interest. Among such materials, we have paid much attention to orthorhombic barium silicide (BaSi<sub>2</sub>) [1,2]. BaSi<sub>2</sub> is composed of abundant chemical elements Si and Ba in the earth's crust, and can be grown epitaxially on a Si(111) substrate by reactive deposition epitaxy (RDE) and molecular beam epitaxy (MBE) [3-6]. The conduction-band minimum and the valence-band maximum are calculated to be at  $T(0\ 1/2\ 1/2)$ , and at around  $(0\ 1/3\ 0)$  along the  $\Gamma$ - $Y(0\ 1/2\ 0)$  direction, respectively [7,8]. The direct transition occurs at around  $(0\ 1/3\ 0)$ , and its gap value is higher than the band gap by approximately 0.1 eV. This might be the reason why the experimental study has revealed that BaSi<sub>2</sub> has a very large absorption coefficient of over  $10^5\ \text{cm}^{-1}$  at 1.5 eV in spite of its indirect band gap nature [9]. In addition, it was found from the optical absorption measurements that the band gap of BaSi<sub>2</sub> can be increased up to approximately 1.4 eV [10,11], matching the solar spectrum, by replacing half of the Ba atoms with isoelectric Sr atoms. This band gap tunability was theoretically supported [8]. Recent reports on the photoresponse properties of BaSi<sub>2</sub> epitaxial layers on Si(111) and polycrystalline BaSi<sub>2</sub> layers on  $\langle 111 \rangle$ -Si layers formed on SiO<sub>2</sub> by the Al-induced crystallization method have shown that BaSi<sub>2</sub> is a very promising Si-based new material for thin-film solar cell applications [12,13]. Control of electron and hole concentrations is possible, and both p-type and n-type BaSi<sub>2</sub> can be realized by impurity doping [14,15]. All these facts suggest that BaSi<sub>2</sub> is promising as a novel material

for thin film solar cells.

However, since there are large conduction and valence band discontinuities at the BaSi<sub>2</sub>/Si heterointerface due to the much smaller electron affinity of BaSi<sub>2</sub> compared with that of Si [16]. Therefore, even when carriers are photogenerated in a BaSi<sub>2</sub> film, they will be blocked at the BaSi<sub>2</sub>/Si interface, thereby significantly decreasing the photocurrent in the external circuit. Formation of an electrical contact between the Si and BaSi<sub>2</sub> is one of the critical steps toward BaSi<sub>2</sub> solar cells on Si. A heavily doped n<sup>+</sup>/p<sup>+</sup> junction that functions as a tunnel junction can be employed to overcome this problem [17]. Recently, we successfully produced heavily-doped n<sup>+</sup>-BaSi<sub>2</sub>/p<sup>+</sup>-Si heterostructure that behaves as a tunnel junction [18]. This tunnel junction enabled us to measure the photoresponsivity of BaSi<sub>2</sub> epitaxial films through the tunnel junction. Furthermore, it was found that the template layer was indispensable for an n<sup>+</sup>-BaSi<sub>2</sub> layer to grow epitaxially on Si(111), and the tunnel resistance increases with increasing undoped template layer thickness [19].

In this paper, we investigated the photoresponse properties of undoped BaSi<sub>2</sub> epitaxial layers grown on n<sup>+</sup>-BaSi<sub>2</sub>/p<sup>+</sup>-Si tunnel junction, and then compared them with those obtained from undoped BaSi<sub>2</sub> layers on a p-Si substrate. The temperature dependence of current density versus voltage (*J-V*) characteristics of the n<sup>+</sup>-BaSi<sub>2</sub>/p<sup>+</sup>-Si tunnel junction was also discussed.

## 2. Experiments

The n<sup>+</sup>-BaSi<sub>2</sub>/p<sup>+</sup>-Si tunnel junction was formed on Si(111) by MBE as follows. The growth temperature for both RDE and MBE was 550 °C. The temperature of Sb was set at 250 °C. First, a heavily Boron doped p<sup>+</sup>-Si layer, approximately 30 nm in thickness, was formed on a p-Si(111) substrate (p~4×10<sup>18</sup>cm<sup>-3</sup>). Then, 1-nm-thick undoped BaSi<sub>2</sub> template layer was formed on the Si substrate by RDE, followed by a 15-nm-thick Sb-doped n<sup>+</sup>-BaSi<sub>2</sub> layer by MBE [19]. Then, a 360-nm-thick undoped BaSi<sub>2</sub> layer, and a 50-nm-thick Sb-doped n<sup>+</sup>-BaSi<sub>2</sub> capping layer were

subsequently grown by MBE (sample A). For comparison, sample without the  $n^+$ -BaSi<sub>2</sub>/p<sup>+</sup>-Si tunnel junction was also prepared (sample B), that is, a 240-nm-thick undoped BaSi<sub>2</sub> film using an RDE-grown 10-nm-thick BaSi<sub>2</sub> template on the p-Si(111) substrate, followed by a 60-nm-thick Sb-doped  $n^+$ -BaSi<sub>2</sub> capping layer. These  $n^+$ -BaSi<sub>2</sub> capping layers allowed the production of ohmic contacts for  $J$ - $V$  measurements. In order to investigate the temperature dependence of  $J$ - $V$  characteristics in an  $n^+$ -BaSi<sub>2</sub>/p<sup>+</sup>-Si diode,  $n^+$ -BaSi<sub>2</sub>(160 nm)/p<sup>+</sup>-Si structure was also prepared on the p-Si(111) (sample C). Samples are summarized as shown in Table 1. For photoresponse measurements, the front-side contacts were made by evaporating 0.5-mm-spaced striped Au/Cr electrodes and the back-side contacts by sputtering Al in samples A and B. Samples were not covered with anti-reflection coatings. For measuring the  $J$ - $V$  characteristics, the 1-mm-diameter front-side contacts were formed by evaporating Au/Cr approximately 150-200 nm in thickness onto the BaSi<sub>2</sub> surface using a metal mask for samples A–C, and the back-side contacts by sputtering Al onto the back of the Si substrate for all the samples.

The crystalline quality of the BaSi<sub>2</sub> was evaluated from reflection high-energy electron diffraction (RHEED) and  $\theta$ - $2\theta$  X-ray diffraction (XRD). The photocurrent in the vertical direction was evaluated using a lock-in technique that employed a Xenon lamp with a 25-cm focal-length single monochromator (Bunko Keiki SM-1700A). The light intensity was calibrated using a pyroelectric sensor (Melles Griot 13PEM001/J).

### **3. Results and discussion**

#### *3.1 Crystalline qualities*

Figure 1 shows the  $\theta$ - $2\theta$  XRD patterns of samples A and B. No peaks other than those from (100)-oriented BaSi<sub>2</sub>, that is, the (200), (400), and (600) planes, were observed, showing that  $a$ -axis oriented BaSi<sub>2</sub> was successfully grown. Figure 2 shows the streaky RHEED patterns of the two samples, which consist of alternating intense and weak streaks, revealing that the  $a$ -axis-oriented BaSi<sub>2</sub> has three

epitaxial variants rotated by  $120^\circ$  to each other in the surface normal direction on Si(111) [20]. These results show that we have successfully formed the  $a$ -axis-oriented 360-nm-thick undoped BaSi<sub>2</sub> layers on the tunnel junction in sample A, and  $a$ -axis-oriented 240-nm-thick undoped BaSi<sub>2</sub> layers on the p-Si in sample B.

### 3.2 $J$ - $V$ characteristics

Figure 3 shows typical examples of  $J$ - $V$  characteristics of samples A and B measured at room temperature (RT) for 1-mm-diameter diodes. The bias voltage was applied to the p-Si substrate with respect to the n<sup>+</sup>-BaSi<sub>2</sub>. Conventional rectifying properties were observed in sample B due to the n-BaSi<sub>2</sub>/p-Si  $pn$  junction diode. In contrast, rectifying properties were not observed in sample A, grown with the tunnel junction, but symmetric  $J$ - $V$  characteristics were observed in the forward and reverse bias conditions. These results show that the n<sup>+</sup>-BaSi<sub>2</sub>/p<sup>+</sup>-Si junction functions as a tunnel junction at the heterointerface. The series resistance of sample A was sufficiently small, being as large as  $0.8 \Omega \cdot \text{cm}^2$  at a bias voltage of 0.1 V at RT. This value is small enough for solar cells. However, we don't have enough information at present to discuss the mechanism of tunneling currents. The temperature dependence of  $J$ - $V$  characteristics was measured on sample C, the n<sup>+</sup>-BaSi<sub>2</sub>/p<sup>+</sup>-Si tunnel junction diode, at temperatures ranging from 90 K to 300 K as shown in Fig. 4. The series resistance increases with decreasing temperature, that is 0.3 and  $1.0 \Omega \cdot \text{cm}^2$  at 300 K and 220 K, respectively, at a bias voltage of 0.1 V. Although several samples displayed negative differential resistance in the  $J$ - $V$  characteristics in the forward bias condition, as is often the case with heavily doped  $n^+/p^+$  Esaki diodes [21], most samples did not. Defect levels are supposed to exist at the n<sup>+</sup>-BaSi<sub>2</sub>/p<sup>+</sup>-Si heterointerface because of the difference in both crystal structure and lattice constants between them. Therefore, we speculate that the tunneling currents flow via localized states in the forbidden gap [22], rather than by a band-to-band direct tunneling. It is important to note that the symmetric  $J$ - $V$  characteristics were observed over the

wide temperature range, and that the series resistance remained negligibly small at temperatures higher than 200 K. Thus, we may say that the electrical properties of the  $n^+$ -BaSi<sub>2</sub>/p<sup>+</sup>-Si junction are satisfactory.

### 3.3 Photoresponse properties

Figure 5 shows the photoresponse properties of sample A under various forward and reverse bias voltages. The direction of the current flow changed between the reverse and forward bias conditions, as shown in Figs. 5 (a) and 5 (b), showing that the applied voltage dropped across the undoped BaSi<sub>2</sub> layers due to the tunnel junction. Light absorption produces electron-hole pairs that are separated by the electric field between the electrodes, which leads to current flow in the external circuit as the photoexcited carriers drift before recombination. Photocurrents were observed for wavelength  $\lambda$  shorter than 1150 nm and increased sharply for  $\lambda$  shorter than 950 nm, reaching a maximum at 500 nm. Wavelengths of 1150 nm and 950 nm correspond roughly to the optical absorption edges of Si and BaSi<sub>2</sub>, respectively. The external quantum efficiency increased up to approximately 17.8% at 500 nm under a reverse bias voltage of 4 V. This value is much larger than that obtained for sample B, discussed later, and also larger than those we have previously reported [12,13]. These results show that a tunnel junction using BaSi<sub>2</sub> was in fact realized. The reason for the negligibly small contribution of photoexcited carriers from the Si, as shown by the photoresponse spectra, is that the photoexcited electrons (minority carriers in p-Si) are likely to recombine with the large number of holes present (ca.  $4 \times 10^{18} \text{ cm}^{-3}$ ) before reaching the electrode.

On the other hand, the external quantum efficiencies of sample B are smaller than those of sample A, as shown in Fig. 6. In addition, the direction of current flow didn't change, meaning that significant amount of the applied voltage dropped across the *pn* junction. Photocurrents were observed for wavelengths shorter than 1150 nm, reaching a maximum at 800 nm. The maximum external

quantum efficiency is only 6.3% at 800 nm under a reverse bias voltage of 2 V, although a certain amount of built-in electric field is used on the BaSi<sub>2</sub>/Si heterointerface. This is probably because of the large conduction and valence band discontinuities at the BaSi<sub>2</sub>/Si heterointerface.

We conclude that a tunnel junction using semiconducting BaSi<sub>2</sub> was in fact realized, and the epitaxial growth of high-quality undoped BaSi<sub>2</sub> layers was accomplished on the tunnel junction. This is really one of the critical steps for the development of BaSi<sub>2</sub> solar cells on Si. Our next target is to form a BaSi<sub>2</sub> *pn* junction diode on the tunnel junction and to demonstrate the solar cell operation.

#### **4. Conclusions**

240-nm-thick undoped BaSi<sub>2</sub> epitaxy films were grown on p-Si(111). Photoresponse spectra for photons with wavelengths shorter than 1150 nm were clearly observed. The external quantum efficiency increased up to approximately 6.3% at 800 nm under a reverse bias voltage of 2 V. 360-nm-thick undoped BaSi<sub>2</sub> epitaxy films were grown on the n<sup>+</sup>-BaSi<sub>2</sub>/p<sup>+</sup>-Si tunnel junction. Photoresponse spectra for photons with wavelengths shorter than 950 nm were clearly observed. The external quantum efficiency increased up to approximately 17.8% at 500 nm under a reverse bias voltage of 4 V. The external quantum efficiency is larger than that obtained for the n-BaSi<sub>2</sub>/p-Si *pn* junction diode. These results show the importance of tunnel junction at the BaSi<sub>2</sub>/Si heterointerface.

#### **Acknowledgements**

This work was supported in part by Grants-in-Aid for Scientific Research B (No. 18360005) from the Ministry of Education, Culture, Sports, Science and Technology of Japan, and PRESTO of the Japan Science and Technology Agency.

## References

- [1] J. Evers, G. Oehlinger, A. Weiss, *Angew. Chem., Int. Ed.* **16** (1977) 659.
- [2] M. Imai, T. Hirano, *J. Alloys Compd.* **224** (1995) 111.
- [3] R. A. McKee, F. J. Walker, J. R. Conner, R. Raj, *Appl. Phys. Lett.* **63** (1993) 2818.
- [4] Y. Inomata, T. Nakamura, T. Suemasu, F. Hasegawa, *Jpn. J. Appl. Phys.* **43** (2004) 4155.
- [5] Y. Inomata, T. Nakamura, T. Suemasu, F. Hasegawa, *Jpn. J. Appl. Phys.* **43** (2004) L478.
- [6] Y. Inomata, T. Suemasu, T. Izawa, F. Hasegawa, *Jpn. J. Appl. Phys.* **43** (2004) L771.
- [7] D. B. Migas, V. L. Shaposhnikov, V. E. Borisenko, *Phys. Status Solidi B* **244** (2007) 2611.
- [8] Y. Imai, A. Watanabe, *Thin Solid Films* **515** (2007) 8219.
- [9] K. Morita, Y. Inomata, T. Suemasu, *Thin Solid Films* **508** (2006) 363.
- [10] K. Morita, M. Kobayashi, T. Suemasu, *Jpn. J. Appl. Phys.* **45** (2006) L390.
- [11] T. Suemasu, K. Morita, M. Kobayashi, *J. Cryst. Growth* **301-302** (2007) 680.
- [12] Y. Matsumoto, D. Tsukada, R. Sasaki, M. Takeishi, T. Suemasu, *Appl. Phys. Express* **2** (2009) 021101.
- [13] D. Tsukada, Y. Matsumoto, R. Sasaki, M. Takeishi, T. Saito, N. Usami, T. Suemasu, *Appl. Phys. Express* **2** (2009) 051601.
- [14] M. Kobayashi, K. Morita, T. Suemasu, *Thin Solid Films* **515** (2007) 8242.
- [15] M. Kobayashi, Y. Matsumoto, Y. Ichikawa, D. Tsukada, T. Suemasu, *Appl. Phys. Express* **1** (2008) 051403.
- [16] T. Suemasu, K. Morita, M. Kobayashi, M. Saida, M. Sasaki, *Jpn. J. Appl. Phys.* **45** (2006) L519.
- [17] D. L. Miller, S. W. Zehr, J. S. Harris, Jr., *J. Appl. Phys.* **53** (1982) 744.
- [18] T. Saito, Y. Matsumoto, M. Suzuno, M. Takeishi, R. Sasaki, T. Suemasu, N. Usami, *Appl. Phys. Express* **3** (2010) 021301.

- [19] T. Saito, Y. Matsumoto, R. Sasaki, M. Takeishi, T. Suemasu, *Jpn. J. Appl. Phys.* **49** (2010) 068001.
- [20] T. Suemasu, M. Sasase, Y. Ichikawa, M. Kobayashi, D. Tsukada, *J. Cryst. Growth* **310** (2008) 1250.
- [21] L. Esaki, *Phys. Rev.* **109** (1958) 603.
- [22] A. G. Chynoweth, W. L. Feldmann, R. A. Logan, *Phys. Rev.* **121** (1961) 684.

Table 1 Preparation of samples A-C. Thicknesses of BaSi<sub>2</sub> template, n<sup>+</sup>-BaSi<sub>2</sub> underlayer, undoped BaSi<sub>2</sub> layer and n<sup>+</sup>-BaSi<sub>2</sub> capping layer are given.

Sample	Substrate	Template (nm)	n <sup>+</sup> -BaSi <sub>2</sub> under layer (nm)	Undoped BaSi <sub>2</sub> (nm)	n <sup>+</sup> -BaSi <sub>2</sub> capping layer (nm)
A	p <sup>+</sup> -Si/p-Si	1	15	360	50
B	p-Si	10	–	240	60
C	p <sup>+</sup> -Si/p-Si	1	160	–	–

## Figure captions

Fig. 1  $\theta$ - $2\theta$  XRD patterns of (a) sample A, grown with the tunnel junction, and (b) sample B, grown without the tunnel junction.

Fig. 2 RHEED patterns observed along Si[11-2] for (a) sample A, grown with the tunnel junction, and (b) sample B, grown without the tunnel junction.

Fig. 3  $J$ - $V$  characteristics of (a) sample A, grown with the tunnel junction, and (b) sample B, grown without the tunnel junction, measured at RT for a 1-mm-diameter. The bias voltage was applied to the p-Si substrate with respect to the n<sup>+</sup>-BaSi<sub>2</sub>.

Fig.4 Temperature dependence of  $J$ - $V$  characteristics measured on sample C.

Fig. 5 Photoresponse spectra of sample A measured at RT for various (a) reverse and (b) forward bias voltages applied between the top and bottom electrodes.

Fig. 6 Photoresponse spectra of sample B measured at RT for various (a) reverse and (b) forward bias voltages applied between the top and bottom electrodes.

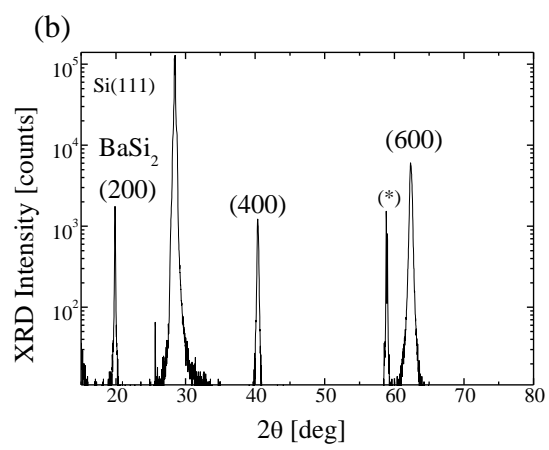
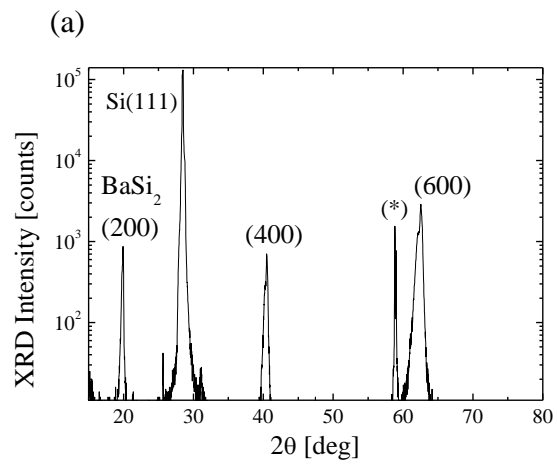


Figure 1

(a)



(b)

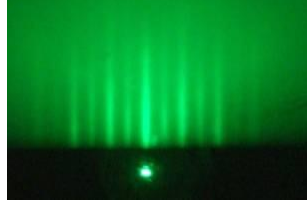


Figure 2

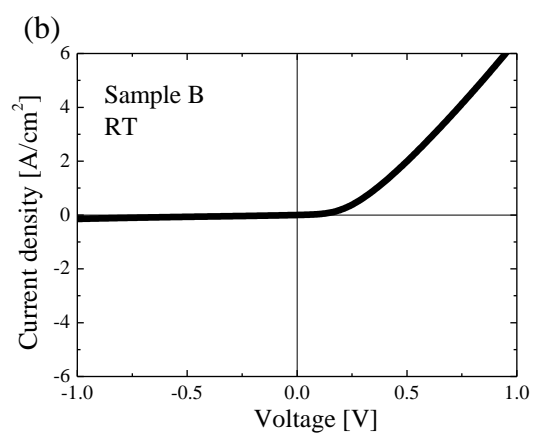
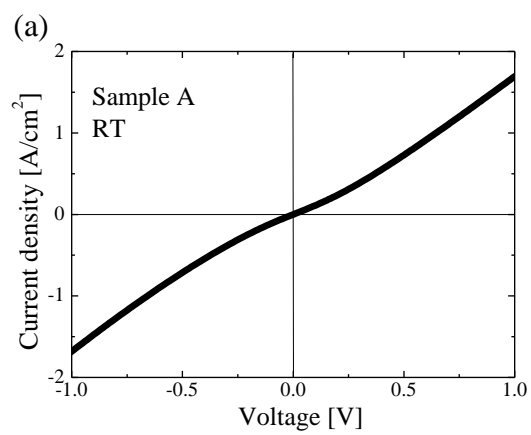


Figure 3

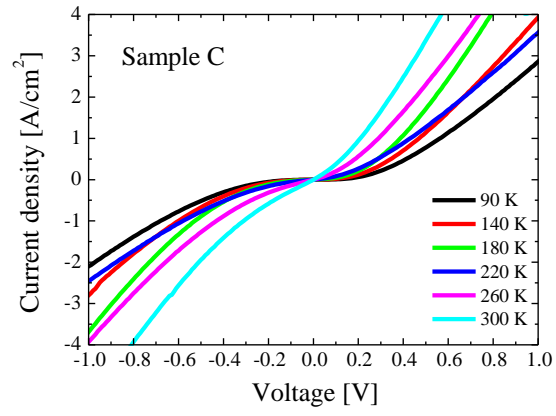


Figure 4

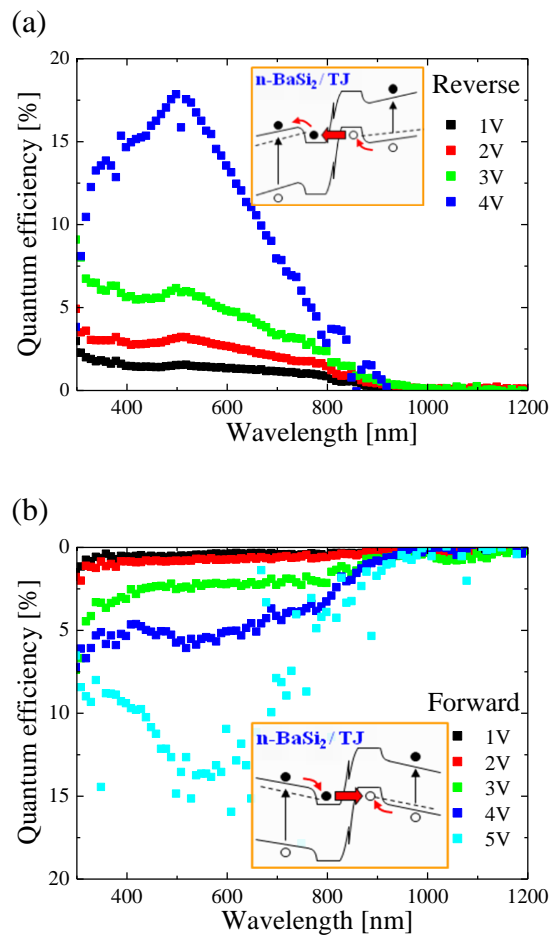


Figure 5

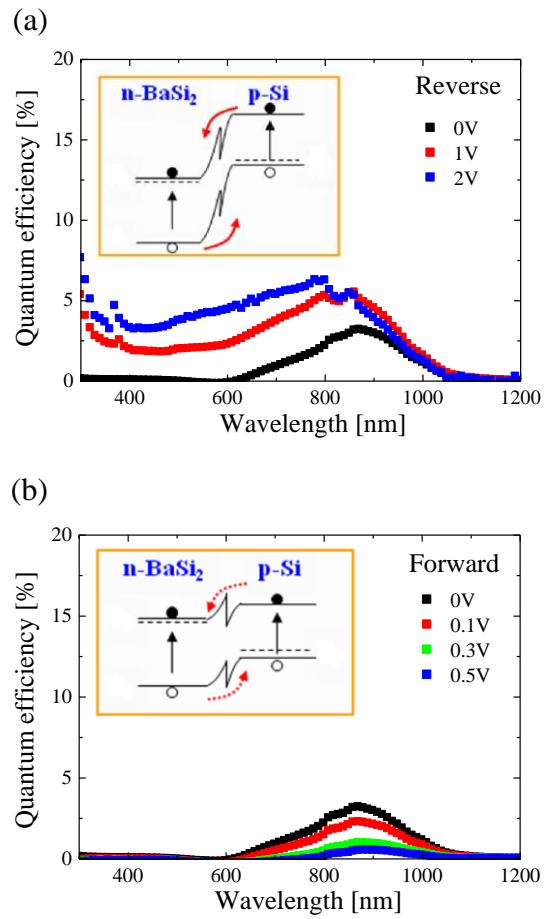


Figure 6